Structural Requirements for Key Residues and Auxiliary Portions of a BLUF Domain[†]

Qiong Wu, Wen-Huang Ko, and Kevin H. Gardner*

Departments of Biochemistry and Pharmacology, University of Texas Southwestern Medical Center, 5323 Harry Hines Boulevard, Dallas, Texas 75390-8816

Received June 23, 2008; Revised Manuscript Received August 6, 2008

ABSTRACT: BlrB in *Rhodobacter sphaeroides* is a single domain, flavin-based blue light sensor protein in the BLUF family of photoreceptors. Consistent with other members of this family, blue light excitation induces a putative signaling state characterized by a 10 nm red shift in the UV−visible absorbance spectrum. Structural and spectroscopic characterization of truncated BlrB constructs establishes that the C-terminal 50 amino acids of this protein are essential to its structural integrity despite not being part of the canonical BLUF domain architecture. Mutagenesis studies support the critical roles of Tyr9, Asn33, and Gln51 for flavin binding and the integrity of the BLUF domain fold. Comparison of solution NMR spectra of BlrB acquired under dark and light conditions indicates very limited light-dependent conformational changes except for a few interesting residues: Trp92, Met94, and Ile127. Notably, the Ile127 side chain experiences significant chemical shift changes despite the fact that it is far (∼15 Å) from the flavin chromophore in the C-terminal extension. These data suggest that the light-induced signal is propagated from the flavin through the β sheet to the last two α helices in the C-terminal extension, potentially providing a mechanism to transmit this change to initiate a cellular response to blue light.

Appropriately sensing and responding to changes in light is critical for many organisms to adapt to their changing environment. In many cases, photoreceptor proteins play the critical role of detecting light of specific wavelengths and controlling downstream signaling in response to this stimulus. Such sensory proteins can be classified into six distinct families: rhodopsins, phytochromes, xanthopsins, cryptochromes, LOV domains, and BLUF[1] domains (*1*). The last three families share the common use of flavin chromophores (FAD or FMN) to detect blue light, although they do so with fundamentally different photochemical and signaling mechanisms. BLUF (sensor for blue light using FAD) (*2*) domains are the newest addition to this group, having been found in bacteria and lower eukaryotes. Based on structures solved by X-ray crystallography and NMR spectroscopy, BLUF domains adopt a $\beta\alpha\beta\beta\alpha\beta\beta$ fold made up of approximately 95 amino acids that envelop the isoalloxazine ring and ribityl chain of a noncovalently bound FAD chromophore (*3*−*5*). Upon absorption of blue light, these domains exhibit a characteristic 10 nm red shift in their UV−visible absorption spectrum (*6*). This shift is believed to indicate the formation of the BLUF signaling state, which spontaneously reverts to the ground state with kinetics that vary from seconds to minutes among different BLUF domains (*7*). Extensive spectroscopic studies have been undertaken to elucidate the photochemistry and signaling mechanism of BLUF domains, leading to the hypothesis that light-induced intramolecular electron/proton transfer and flavin/protein hydrogen-bonding rearrangement are thought to initiate the signaling state formation (*6, 8, 9*). However, the molecular details of this intriguing process are still poorly understood.

BlrB (blue light receptor B, 140 amino acids), one of the three BLUF-containing proteins from *Rhodobacter sphaeroides*, belongs to a class of "short" single domain proteins that contain a single BLUF domain as the only recognizable domain within its sequence. BlrB has a canonical BLUF domain at its N-terminus, followed by an additional 50 C-terminal amino acids of unknown function. Crystallographic structure determination (*4*) and visible spectroscopy (*7*) have shown that BlrB adopts a typical BLUF domain fold and displays characteristic changes in the UV−visible absorbance spectrum upon blue light excitation. However, both the biological function and signal propagation process of BlrB remain unknown, as the C-terminal extension shows no evidence of catalytic activity and no binding partners have been identified.

To gain further insight into the structural and signaling roles of BlrB, we used a combination of biophysical and biochemical methods to examine the importance of the C-terminal extension and several key amino acids within this protein. We characterized several different forms of BlrB truncated at various C-terminal sites, finding that the structural integrity and proper photoproduct formation of the BLUF domain are dependent on the extension outside the canonical BLUF domain. In addition, we constructed point mutants of BlrB, targeting residues implicated in its flavin binding and photochemistry, and found that these changes alter the photocycle or preclude flavin binding

[†] This work was supported by a grant from the Robert A. Welch Foundation (I-1424) to K.H.G.

* Corresponding author. Phone: 214-645-6365. Fax: 214-645-6353. E-mail: Kevin.Gardner@utsouthwestern.edu.

[1] Abbreviations: BLUF domain, sensor for blue light using FAD; BlrB, blue light receptor B.

10.1021/bi8011687 CCC: $40.75
Published on Web 09/05/2008

entirely. Finally, we studied the conformational changes that take place in BlrB upon blue light excitation using solution NMR spectroscopy. Comparisons of NMR data acquired under dark and light conditions suggest that BlrB undergoes very limited structural changes upon blue light illumination, although several residues exhibit relatively large light-dependent chemical shift changes. While the majority of these sites are within the flavin-binding pocket, a few are located outside of the canonical BLUF fold at the two C-terminal α helices, 15 Å or more away from the chromophore. These observations provide evidence of remote light-induced structural changes and lead us to discuss the possible BLUF domain architecture and the signal transduction pathway.

MATERIALS AND METHODS

Sample Preparation. DNAs encoding the full-length BlrB, BlrB(1−116), BlrB(1−122), BlrB(1−130), and BlrB(1−135) sequences were subcloned into the pHis-Gβ1-parallel expression vector (*10*). *Escherichia coli* BL21(DE3) cells transformed with these plasmids were grown in M9 media containing 1 g/L $^{15}NH_4Cl$ for U-^{15}N samples and supplemented with 3 g/L $^{13}C_6$-glucose for U-^{15}N/^{13}C-labeled samples. Cultures were grown at 37 °C to A_{600} ~0.7 and then induced overnight at 20 °C by the addition of 0.5 mM isopropyl β-D-thiogalactoside. Cells were harvested and the resulting pellets resuspended in 50 mM Tris (pH 8.0) and 100 mM NaCl buffer and lysed by extrusion. Lysates were clarified by centrifugation at 10000*g* for 30 min. The supernatant was loaded onto a Ni^{2+}-NTA column, allowing the rapid affinity purification of His-Gβ1-tagged BlrB by eluting with 250 mM imidazole. After exchanging BlrB-containing fractions into 50 mM Tris (pH 8.0) buffers, the His-Gβ1 tag was cleaved by adding 1 mg of His_6-TEV protease (*11*) per 30 mg of protein. The His-Gβ1 tag and His_6-TEV protease were removed from BlrB (containing an N-terminal GEF cloning artifact followed by the BlrB sequence) by passing over Ni^{2+}-NTA again. Purified BlrB was then exchanged into the final buffer, 50 mM Tris (pH 8.0) and 30 mM NaCl, and concentrated to 50 μM for UV−visible absorbance spectroscopy experiments, 100 μM (for dark vs light NMR experiments), and 900 μM (for chemical shift assignment experiments) for solution NMR experiments.

Mutation. Point mutants of BlrB were generated from wild-type DNA and primers including the desired mutations by QuickChange (Stratagene) PCR amplification. The following mutants were obtained: Y9F, Y9W, Y9L, A28I, A28T, R32K, R32N, R32H, N33Q, N33D, N33V, Q51E, Q51N, Q51L, L66W, and L66F. All amino acid changes were verified by DNA sequencing. Transformation, protein induction, and purification were performed in the same fashion for wild type as described above. Postillumination dark state recovery rates at 25 °C were measured at 446 nm for all mutants that bound flavin cofactors.

NMR Spectroscopy. All NMR experiments were performed at 25 °C on Varian Inova 500, 600, and 800 MHz spectrometers, using nmrPipe for data processing (*12*) and NMRview for analysis (*13*). Dark state backbone chemical shift assignments were obtained using standard 3D ^{15}N-edited triple resonance experiments (*14*) including HNCACB, CBCA(CO)NH, HNCO, ^{15}N-edited NOESY (τ_m = 120 ms), and simultaneous ^{15}N,^{13}C-edited NOESY (τ_m = 120 ms) experiments. Aliphatic side chain resonances were assigned from HCCH-TOCSY, HC(CO)NH-TOCSY, and C(CO)NH-TOCSY spectra. Secondary structure was predicted by TALOS analysis (*15*) of backbone ^1H, ^{13}C, and ^{15}N chemical shifts.

To obtain NMR spectra of the photoexcited state of BlrB, we generated blue light from a Coherent Inova-90C argon laser running in single wavelength mode at 457 nm and directed this into a quartz fiber optic inserted into the NMR sample (*16*). Power levels at the end of this fiber were 120 mW as measured before each experiment. ^{15}N/^1H and constant time ^{13}C/^1H HSQC spectra of the light state of BlrB were recorded by preceding each transient in the NMR experiment with the application of a 200 ms laser pulse during the recycle delay (a total of 1060 ms delay between scans).

Due to its rapid dark state recovery rate (*7*) and significant absorbance of light at 457 nm in both the dark and light states, a substantial amount of light is needed to populate the BlrB photoproduct state. We confirmed the reversibility of the BlrB photochemistry by comparison of UV−visible absorbance and NMR spectra recorded before and after illumination. These studies indicated that significant irreversible bleaching occurred only after approximately 3 h using the protocol described above, precluding full assignment of light state chemical shifts by standard methods. Thus, all of the light state chemical shift assignments of BlrB were done by transferring the assignments of any newly observed peaks in NMR spectra from the nearest disappearing peak, which was possible for about 12 CH_3 sites.

UV−Visible Absorbance Spectroscopy. All UV−visible absorbance spectra were acquired using a Cary 50 (Varian) spectrophotometer. Samples were photoactivated using a photographic flash. Dark state recovery of the flavin cofactor was monitored by the changes in the absorbance at 446 nm after illumination, recording A_{446} every 1 s with an integration time of 0.1 s. Rates were determined by averaging the fit of four separate measurements to a single exponential decay. A circulating water bath was used for temperature control of the sample in a quartz cuvette. Experiments were conducted at 5 °C increments from 5 to 30 °C. Solvent isotope effect experiments were conducted in 50 mM Tris (pH 8) and 30 mM NaCl in D_2O, and data were recorded at 5 °C increments between 10 and 30 °C. Arrhenius analysis of the temperature dependence of dark state recovery rates ($\ln(k)$ vs $1/T$) was carried out for direct comparisons of the activation energies of this process.

RESULTS

BlrB Domain Architecture. Sequence alignments of BLUF domains have suggested that the canonical BLUF domain contains approximately 95 amino acid residues. This prediction has been supported by structural studies of several BLUF domains, all of which share a similar $\beta\alpha\beta\beta\alpha\beta\beta$ fold for this conserved region (*3*−*5*, *17*). To investigate the role of the ~50 residues located to the C-terminal side of the BlrB BLUF domain, we generated four C-terminal deletion constructs named BlrB116, BlrB122, BlrB130, and BlrB135, with the most C-terminal residue as indicated and the full-

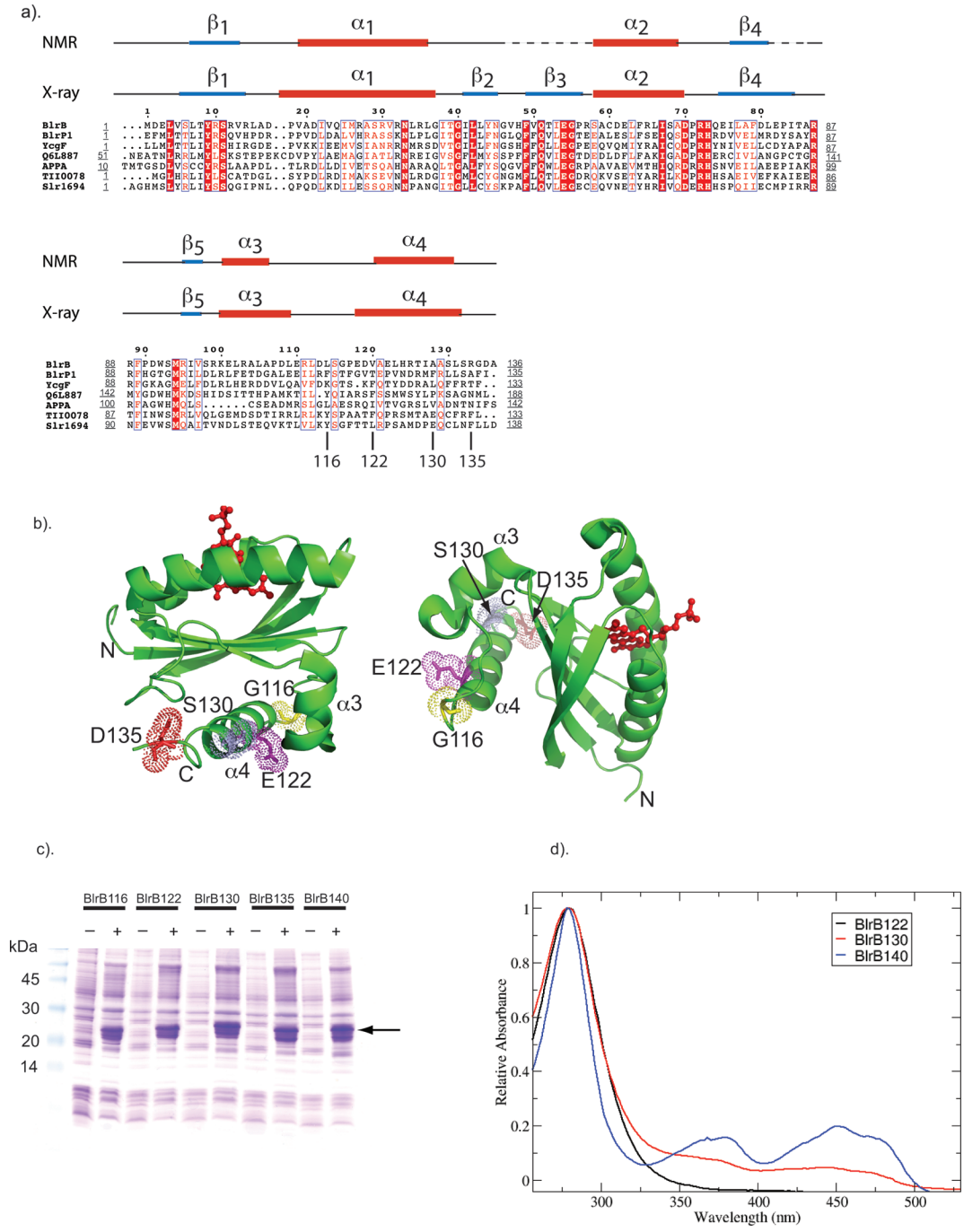

FIGURE 1: Sequence alignment of BLUF proteins and BlrB constructs. (a) Multiple sequence alignment of a selection of BLUF domains as identified by a hidden Markov model search (*33*). Red shaded characters indicate identical residues, while red characters indicate conserved residues. Beginning and end points of each sequence within the native sequences are listed. Key: BlrB, full length from *R. sphaeroides* BlrB; BlrP1, residues 1−133 from *K. pneumoniae* BlrP1; YcgF, residues 1−132 from *E. coli* YcgF; Q6L887, residues 51−188 from *C. sideropus* Q6L887; AppA, residues 10−142 from *R. sphaeroides* AppA; Tll0078, full length from *T. elongates* Tll0078; Slr1694, residues 1−138 from *Synechocystis* Slr1694. Secondary structure elements as observed in the BlrB X-ray structure (PDB: 2BYC (*4*)) and from our NMR data are shown above the BlrB sequence, including a dashed line for residues without chemical shift assignments. (b) Two views of the BlrB X-ray structure (*4*), showing the location of the C-terminal boundaries of each of the truncated BlrB constructs. Residue number and type are as labeled. (c) SDS−PAGE gel of *E. coli* cell lysates showing the induction levels of full-length BlrB and four C-terminal truncated constructs. "−" and "+" represent lanes with lysates of cells harvested before and after induction, respectively. We occasionally observed doublets of overexpressed protein as documented here, with the top band corresponding to the proper length of the protein. (d) UV−visible absorbance spectra for BlrB122, BlrB130, and BlrB140 (BlrB135 has similar absorbance spectrum as BlrB140, not shown).

length protein being BlrB140 (Figure 1a,b). BlrB116 was truncated in the loop connecting the α_3 and α_4 helices in the C-terminal region, BlrB122 ended at the first residue of the α_4 helix, BlrB130 stopped in the middle of α_4, and BlrB135 had two more residues following α_4. Of the four C-terminal deletion constructs, BlrB116 had relatively poor solubility and stability during purification; BlrB122 and BlrB130 expressed well but exhibited little or no flavin binding (Figure 1c,d). BlrB135 bound to flavin as expected, but the protein was less stable than the full-length BlrB shown by decreasing peak intensities in $^{15}N/^{1}H$ HSQC experiments collected while the protein was incubated at room temperature (not shown).

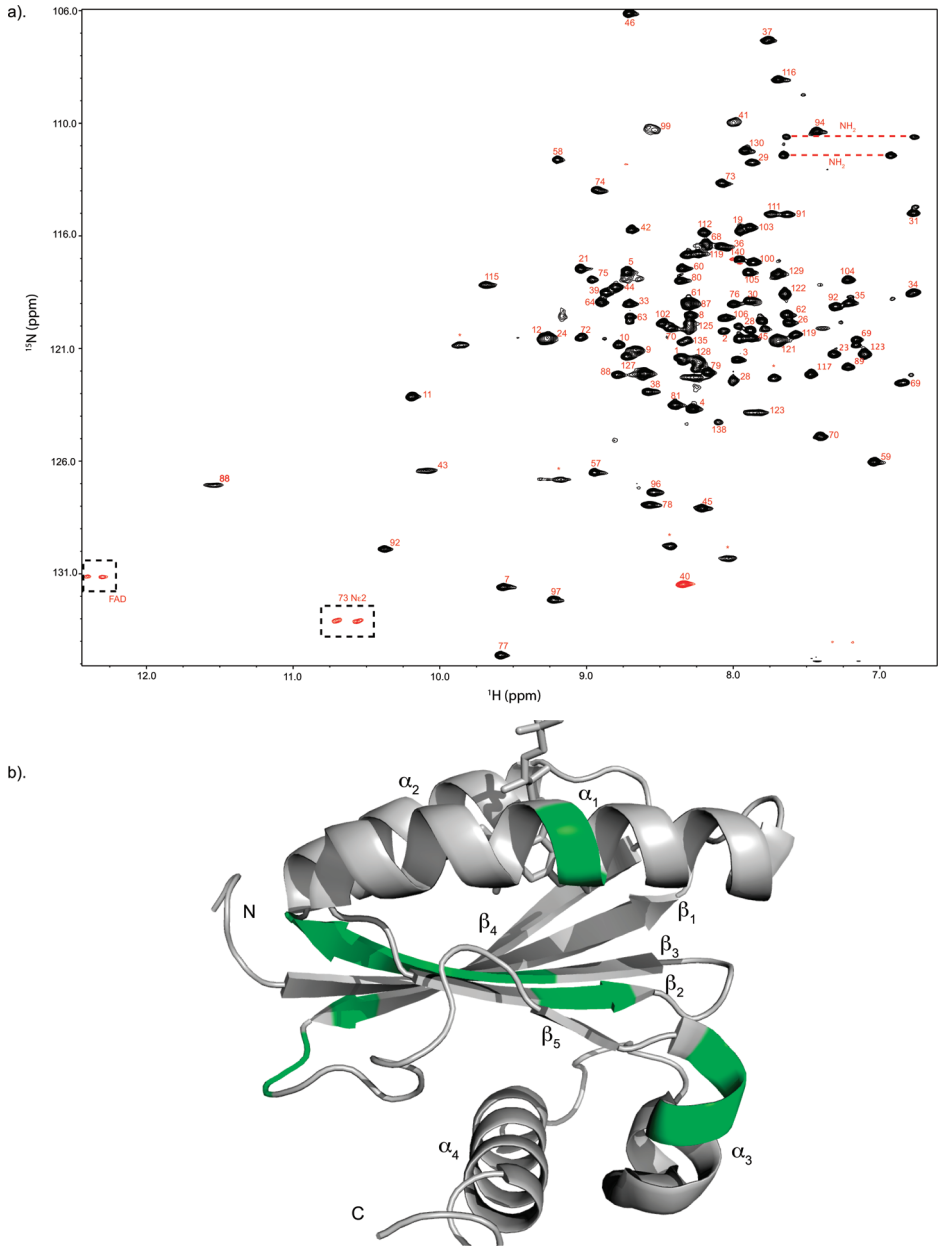

FIGURE 2: BlrB chemical shift assignments. (a) ^{15}N−^{1}H HSQC spectrum and peak assignments of dark state BlrB. Red peaks are aliased in the indirect ^{15}N dimension, some of which exhibit splitting in the ^{1}H dimension due to insufficient ^{15}N decoupling strength. Unassigned peaks are indicated with an asterisk (*) or with NH_2 to designate side chain amides. (b) Unassigned residues (green) are mapped on the X-ray structure of BlrB (*4*). These are mainly confined to residues 50−57 (β_3 strand), 82−85 (β_4 strand), and 99−101 (α_3 helix). Secondary structure elements are as labeled.

Thus, our data demonstrated that these extra residues outside of the canonical BLUF domain are critical to the structural integrity and flavin binding characteristics of BlrB. On the basis of these results, we focused our further studies exclusively on the full-length BlrB protein.

NMR Chemical Shift Assignment. Out of 140 residues, we were able to assign 80% of backbone and 60% overall ^{15}N, ^{13}C, ^{1}H chemical shifts in full-length BlrB. Secondary structure elements were identified with TALOS analysis of backbone chemical shifts (*15*) and verified by ^{1}H−^{1}H NOEs. These predicted secondary structures agree very well with published X-ray structures of BlrB and other BLUF domain proteins (Figure 1a) (*4*). Notably, we were unable to assign chemical shifts for several short regions (residues 50−57, 82−85, and 99−101), due to approximately 10 amide ^{1}H−^{15}N pairs missing from the ^{15}N/^{1}H HSQC spectrum or accompanying triple resonance spectra used for chemical shift assignments (Figure 2). The reason for these missing peaks and chemical shift assignments is not entirely clear, but we suggest two possible reasons here. First, we acquired our NMR data under mildly basic conditions (pH 8). At this pH, base-catalyzed amide proton exchange with solvent could cause peak broadening, especially for solvent-accessible sites. However, we also suggest that intermediate time scale chemical exchange processes may contribute to the broadening given that some of the missing residues, e.g., residue 50−57, are predicted to be buried in stable secondary structure (β_3 strand) in the protein core. Intriguingly, residues 50−57 that form the β_3 strand are located immediately underneath the isoalloxazine ring of flavin. Similar peak broadening for residues in the nearby β_5 strand was also reported in NMR studies of the AppA BLUF domain (*18*).

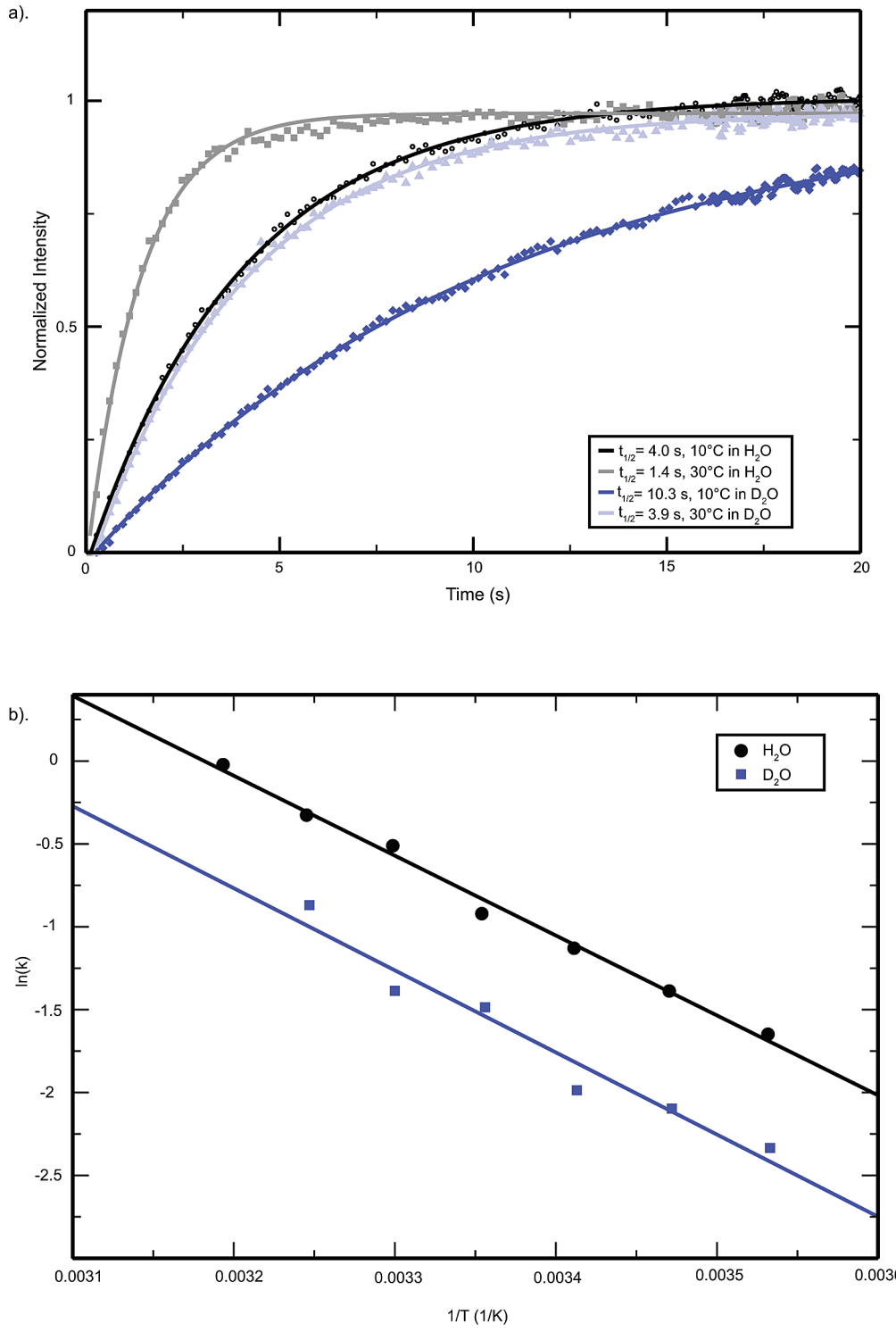

FIGURE 3: Dark state recovery kinetics of BlrB. (a) Dark state recovery of BlrB monitored at 446 nm in H_2O and D_2O at 10 and 30 °C (H_2O, 10 °C = black; H_2O, 30 °C = gray; D_2O, 10 °C = dark blue; D_2O, 30 °C = light blue). Data were fit to single exponential decay functions using the program xmgrace (*34*). (b) Arrhenius plot of BlrB in H_2O and D_2O. Activation energy is calculated by $k = Ae^{-E_a/RT}$. Our observation of parallel plots in H_2O and D_2O indicates that the activation energy of BlrB is not affected by $^1H/^2H$ exchange.

Dark State Recovery of BlrB. Kinetic studies show that all BLUF domains studied to date have a similar, rapid rate of signal state formation on a 100 ps time scale (*8*). It is then notable that different BLUF domain proteins have dark state recovery rates that vary over several orders of magnitude, ranging from $t_{1/2}$ ~15 min for the multidomain BLUF protein, AppA (*19*), to $t_{1/2}$ ~5 s for several isolated BLUF-only proteins (*7, 20*). Our data indicated that BlrB undergoes the signature 10 nm red shift upon illumination (*4*) and that the photoexcited BlrB quickly returned to the dark-adapted state ($t_{1/2}$ = 4.0 s at 10 °C) (Figure 3a). Similar dark state recovery experiments conducted in D_2O showed that the rate in D_2O was 2.5-fold slower than in H_2O ($t_{1/2}$ = 10.3 s at 10 °C). This is comparable to the isotope effect reported for another BLUF domain Slr1694 (*20*). Arrhenius plot analyses showed that the activation energy of BlrB is not affected by $^1H/^2H$ exchange (E_a = 9.6 kcal mol^{-1} in H_2O and E_a = 9.8 kcal mol^{-1} in D_2O) (Figure 3b). These results indicate that

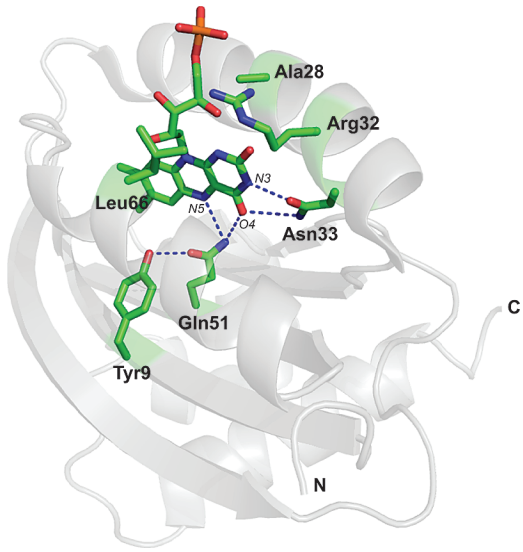

FIGURE 4: The flavin-binding pocket of BlrB. Mutated amino acid sites of BlrB on the X-ray structure: Tyr9, Ala28, Arg32, Asn33, Gln51, and Leu66. Hydrogen bonds are drawn with dashed lines.

Table 1: Summary of Flavin-Binding and Photochemical Properties of BlrB Mutants

point mutant	FAD binding[a]	photocycling[a]	$t_{1/2}$ (s) at 25 °C[b]
Y9F	no	no	nd[c]
Y9W	yes	no	nd
Y9L	no	no	nd
A28I	yes	yes	2.39
A28T	yes	yes	2.39
R32K	yes	yes	2.38
R32N	yes	yes	2.16
R32H	yes	yes	1.30
N33Q	no	no	nd
N33D	no	no	nd
N33V	no	no	nd
Q51E	no	no	nd
Q51N	no	no	nd
Q51L	no	no	nd
L66W	yes	yes	1.52
L66F	yes	yes	0.72
WT	yes	yes	4.17

[a] FAD binding and photocycling of BlrB mutants were verified by UV−visible absorbance spectra. [b] Dark state recovery rates of BlrB mutants were monitored at 446 nm with 50 μM protein in a buffer of 50 mM Tris (pH 8.0) and 30 mM NaCl. [c] nd, not determined.

the slowing of dark state recovery in D_2O is not due to the conformational change of BlrB but rather that a critical step of recovery involves proton transfer or hydrogen bond rearrangement. These results are consistent with the results from biophysical studies of other BLUF domains (*6*).

BlrB Mutants. Two possible photoactivation pathways have been recently proposed for BLUF domains (*3, 4*). On the basis of the BlrB X-ray structure and quantum chemical calculations on lumiflavin, Jung et al. (*4*) proposed that excitation initiates changes in the hydrogen-bonding network around O2 of the ribityl chain. Further, they suggested that light-induced changes in the flavin would be mediated through Arg32 to the surface of the protein (*4*). Anderson et al. suggested an alternative photoactivation mechanism of the AppA BLUF domain involving reorientation of the conserved Gln63 side chain (Gln51 in BlrB) to form an altered protein−chromophore hydrogen-bonding network, subsequently inducing a global structural change (*3*). Examination of the BlrB X-ray structure indicates that several key residues conserved among BLUF domains (Tyr9, Asn33, and Gln51) are in close proximity to the FAD chromophore (Figure 4) (*4*). All three of these residues make hydrogen bond interactions with the flavin isoalloxazine ring and are highly conserved among BLUF domains, suggesting that they have some importance for FAD binding and the BLUF domain photocycle. On the basis of this observation, we made point mutations of BlrB at sites Tyr9, Asn33, and Gln51 and at residues within the α_1 and α_2 helices on the protein surface (Ala28, Arg32, and Leu66) (Figure 4). We speculated that any perturbation on the signaling pathway would alter the structural and correspondingly spectral consequences of photoactivation. Furthermore, the different effects from these mutants would give us clues to validate the two proposed signal transfer pathways (*3*).

A comparison of the FAD-binding ability and photochemical properties of BlrB variants containing point mutations at these sites is provided in Table 1. Our data support structural studies that show that two key residues, Asn33 and Gln51, play absolutely essential roles for flavin binding and photochemistry of BlrB. Notably, these two residues directly hydrogen bond with the flavin isoalloxazine ring (*4*) and cannot tolerate any of the mutations we have made. All mutations for these two residues completely abolish BlrB's flavin-binding capacity and photocycling ability, even for very conservative changes that simply insert/remove a single side chain methylene group (e.g., N33Q, Q51N). These data indicate that the orientation and positions of the side chain amides of these residues are absolutely essential to forming protein/flavin interactions that involve hydrogen bonds to the N3, O4, and N5 positions. Tyr9, whose hydroxyl group is believed to orient Gln51 for proper hydrogen bonding with flavin (*3*), also significantly contributes to the stability of these interactions as demonstrated by the ability of the Y9F and Y9L mutants to disrupt flavin binding as effectively as the N33 and Q51 mutants. Notably, while Y9W still binds to flavin, it does not photocycle after light excitation (or the photocycle is accelerated beyond detection, $t_{1/2} < 0.1$ s). This implies that, at that particular location, BlrB needs hydrogen-bonding functionality which Y9W can provide but Y9L and Y9F cannot. Notably, different BLUF domains show different dependencies on these important residues. For example, Y21L, Y21F (*6*), and Q63L (*21*) of AppA bind flavin normally but did not exhibit any change in visible absorbance spectrum upon illumination. The same case was observed for Q52A of Tll0078; however, its N31A and N32A point mutants behaved essentially as wild type with different dark state decay rates (*17*).

Arg32, a less conserved residue among BLUF domains (His for AppA, Asn for Slr1694. and Asn for Tll0078) that forms direct hydrogen bonds with the 3′-hydroxyl oxygen of the flavin ribityl chain, shows a less critical role in terms of structural integrity and photochemistry. Three mutants of Arg32 (R32K, R32H, and R32Q) bind flavin properly and undergo the characteristic 10 nm red shift upon illumination. These data demonstrate that hydrogen bonding to Arg32 does not affect flavin photochemistry.

In our studies, all mutants other than mentioned above show relatively minor effects. All of the mutants of Ala28 (A28I and A28T) and Leu66 (L66W and L66F) bound flavin and had similar photochemical properties as the wild-type

protein. However, their dark state recovery rates increased by 1.5−6-fold compared with wild type. R32K and R32Q have similar dark state recovery rates, both of which roughly 2-fold faster than the wild-type BlrB. R32H, however, decays to the dark state 4-fold faster than the wild type. Intriguingly, this agrees with the report that significant concentrations of imidazole (imidazole = 2 M) accelerate the ground state recovery of the photoexcited AppA BLUF domain (*22*). L66F shows the fastest dark state recovery rate among all of the mutants we have characterized. Notably, L66F is located on the surface of BlrB, far from the flavin binding pocket, suggesting this mutant indirectly changes BlrB structure and dynamics near the chromophore pocket. Further studies are needed in order to understand the accelerated dark state recovery process by these various mutants, e.g., whether it is any specific interference to the signaling process or the mutations simply destabilize the protein, thus increasing its solvent accessibility.

Solution NMR Studies of Dark and Light States of BlrB. We used solution NMR spectroscopy to further investigate the effect of photoexcitation on BlrB at the residue level. Both dark and light NMR spectra of BlrB (Figure 5) were monitored at backbone amide and side chain methyl groups using ^{15}N/^{1}H and constant time ^{13}C/^{1}H HSQC spectra. Using triple resonance NMR methods, we were able to assign 134 peaks in the ^{15}N/^{1}H HSQC spectrum (Figure 2), roughly 10−15 peaks short of those expected from the amino acid sequence. Overall, our results establish that BlrB itself does not undergo large conformational changes upon illumination, compatible with reports from several other BLUF domains (*3, 20*). For NH backbone resonances, the dark and light state spectra were almost superimposable, with few substantial chemical shift changes upon light excitation. However, illumination reduced peak intensities throughout the spectrum. The magnitude of this effect varied widely, ranging from 10% reduction to complete disappearance. These effects were reversible by allowing the protein to recover in the dark for 30 s or longer, ruling out precipitation as one source of these decays. A comparison of ^{15}N backbone amide T_1 and T_2 relaxation rates in dark and light states revealed similar values and correspondingly similar rotational correlation times that were consistent with monomeric protein (dark state $\tau_c = 8.2 \pm 0.5$ ns, light state $\tau_c = 8.5 \pm 0.5$ ns) (*23*). This suggests that light excitation does not lead to significant tertiary structural changes in the solution properties of BlrB. As such, the decrease in peak intensity arises from reasons other than dimerization, e.g., by inducing motions at different dynamics regions after light excitation or increasing solvent exchange.

In contrast, the methyl region of ^{13}C/^{1}H HSQC spectra recorded under dark and light conditions displayed somewhat larger effects on peak locations and intensities. In particular, these spectra exhibited more slow-exchange type shifts in peak location, rather than simple peak disappearance. While we were able to assign the chemical shifts of 67 methyl groups (out of 81 total) in the dark state using triple resonance methods, this approach was not feasible in the light state due to poor sample behavior. As a result, we can assign sites that are affected by illumination by the disappearance of their dark state peaks, but their corresponding light state peak locations can only be tentatively assigned by assuming that the new light state peaks correlate with

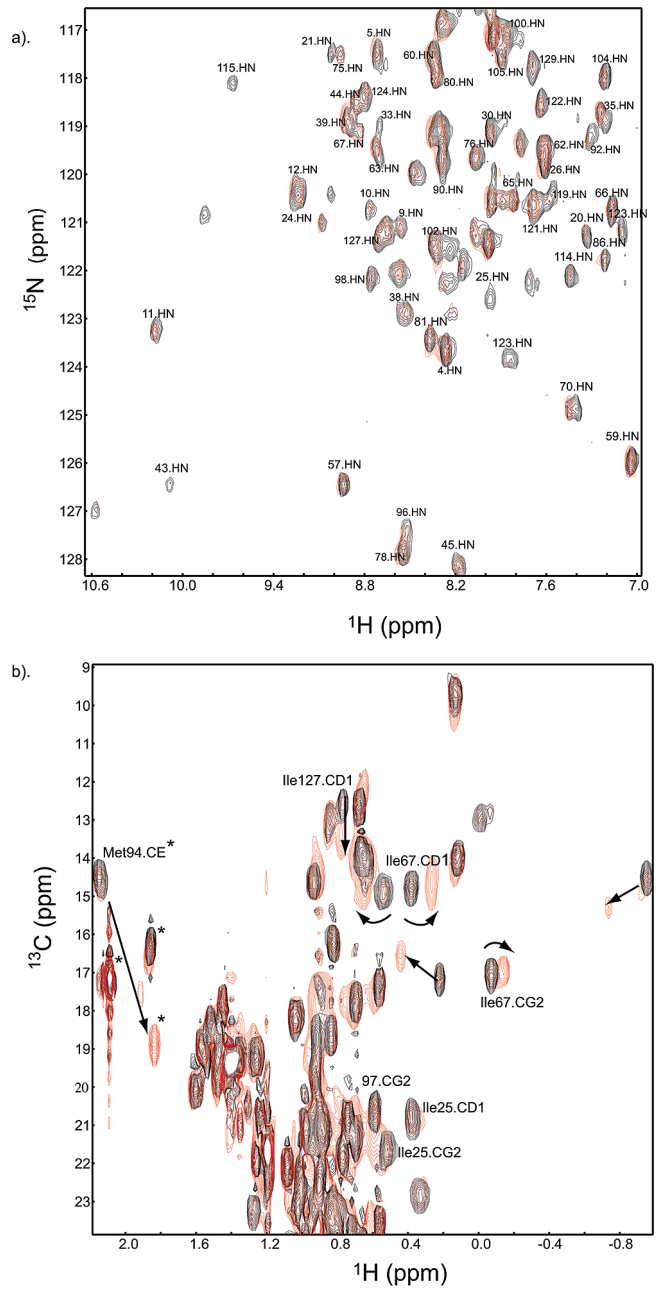

FIGURE 5: ^{15}N/^{1}H and ^{13}C/^{1}H HSQC spectra of BlrB under dark and light conditions. (a) Dark (black) vs light (red) ^{15}N/^{1}H HSQC spectra of BlrB. Peak intensities across the spectrum are differentially decreased upon light illumination, ranging from ∼10% to 100% decrease. (b) Methyl region of dark (black) vs light (red) constant time ^{13}C/^{1}H HSQC spectra of BlrB. Peaks with negative intensity, corresponding to Met Cε methyl groups, are indicated with an * (three Met total). Residues with relatively large chemical shift change are labeled with the assignments where available.

the nearest dark state partners. Those residues are mapped on the BlrB structure as shown in Figure 6. As expected, most residues are within the flavin binding pocket, surrounding the isoalloxazine ring of flavin, where illumination would be expected to cause the large changes of the local chemical environments. These sites include Met94, which is highly conserved among BLUF domains and shows the most significant change (∼0.5 ppm ^{1}H, ∼2 ppm ^{13}C) upon light illumination. In the BlrB crystal structure, the methyl group of Met94 is in the vicinity of isoalloxazine ring, adjacent to the C4/O4 carbonyl group. Met94 also orients Trp92, a residue that is the subject of significant debate for its

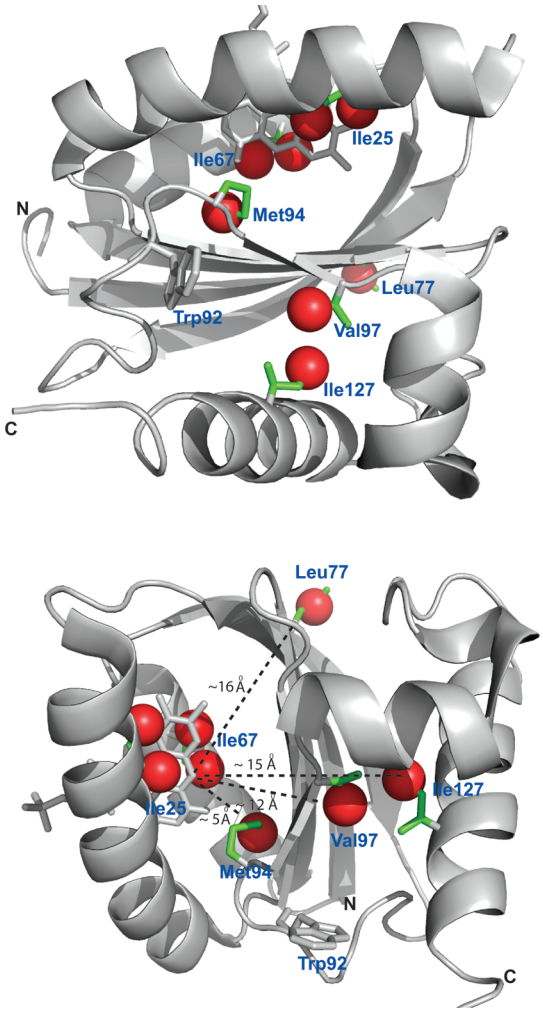

FIGURE 6: Sites showing light-dependent changes in BlrB. Methyl groups showing significantly changed peak location or intensities in CT $^{13}C/^{1}H$ HSQC were mapped on the BlrB X-ray structure. The sites shown are Ile25•Cγ_2, Ile25•Cδ_1, Ile67•Cγ_2, Ile67•Cδ_1, Ile77•Cγ, Met94•Cε, 97•Cγ_2, and Ile127•Cδ_1. The Trp92 side chain (gray) is shown to illustrate the relative positions of Trp92 and Met94.

important role as the signaling switch in BlrB and other BLUF domains (*24, 25*). Notably, several sites outside of the flavin-binding pocket show significant changes. These include Ile127 $C_{\delta 1}$ and Val97 $C_{\gamma 1}$, both of which are located under the β sheet at considerable distances from the flavin (>10 Å for Val97, >15 Å for Ile127) (Figure 6). This suggests that the C-terminal α-helical extension, which we showed to be critical for BlrB structural integrity, is affected upon illumination.

DISCUSSION

BlrB exists as a monomer under dark state conditions as determined by NMR relaxation experiments and gel filtration chromatography (data not shown). This contrasts with several other BLUF containing proteins, particularly AppA. The three different constructs of AppA were reported as dimers in solution (*3, 18, 26, 27*). However, the C termini of those three constructs do not include the presumed BlrB-equivalent third α helix. The absence of this α helix may prevent AppA from properly folding, exposing the highly hydrophobic β sheet for dimerization. This is supported by crystal structures of the AppA BLUF domain, which show a detergent-mediated dimer via this region (*3*). Secondary structure predictions carried out using both Jpred (*28*) and PROF (*29*) indicate that AppA may have two additional C-terminal α helices immediately after its BLUF domain, consistent with our observation for BlrB. For BlrB, the two well-folded α_3 and α_4 helices dock under and tightly attach to the β sheet, protecting the hydrophobic interface and proving essential for the stability of this particular protein. Two similar α helices were also found in crystallographic structures of full-length Slr1694 and Tll0078 (*5, 17*) despite their highly diverse amino acid sequences, suggesting that the C-terminal α helices may have a common role in signal transduction among BLUF domain proteins. In summary, these data seem to support the model for transduction via the β sheet surface (*27*) as opposed to the α-helical surface or ribityl chain. A definitive understanding of this process will require functional characterization of BlrB (and other small BLUF-only proteins), which will hopefully identify the binding surfaces used by their partner proteins and potentially also provide some insight into the related question of the role of the adenine moiety that is unique to FAD (versus FMN).

Grinstead and colleagues (*18*) have shown that residues clustered on the β sheet display significant chemical shift changes in AppA upon light excitation and are likely to be the interface propagating the light-induced structural signal. Thus, it is important to get probes further away for a large aromatic chromophore, allowing us to clearly identify *bona fide* changes resulting from protein conformational changes rather than simply configurational alterations of the isoalloxazine ring. Such data are provided here by our observations of widespread peak intensity reductions in the $^{15}N/^{1}H$ HSQC spectrum and long-range chemical shift changes in $^{13}C/^{1}H$ spectra (Figures 5 and 6). An interesting comparison is provided by another flavin-bound blue light photoreceptor, the LOV domain. Previous studies in our laboratory identified a new structural component outside the canonical LOV core of the *Avena sativa* phototropin1 LOV2 domain, termed as the Jα helix (*10*). This helix covers the otherwise solvent-exposed face of the LOV2 β-sheet in the dark but is displaced by photochemically initiated conformational changes within the LOV2 domain. An analogous mechanism has been described for the *Neurospora crassa* LOV-containing protein, Vivid, despite significant differences in the sequence and structure of elements outside the conserved LOV region (*30*). Taken together, these data suggest that BLUF and LOV domains may share interesting parallels in signal transduction despite their differences in their sequences, overall topology, and photochemistry.

Of particular interest in BLUF structure and signaling is a tryptophan located near the isoalloxazine ring in BlrB and its analogues (*25, 27, 31*). This tryptophan residue, Trp92 in BlrB, is highly conserved among BLUF domains and adopts one of two different conformations in various structures, being either buried inside the protein core (PDB codes: 2HFN and 1YRX) or solvent-exposed (PDB: 2BYC, 2HFN, and 1XOP). This residue is located in the β_5 strand, which shows extensive dynamic behavior among BLUF domains (*18, 25*). In the single-domain BLUF protein Slr1694 (*5*), the analogous Trp91 residue is observed in a

solvent-exposed orientation in nine of the ten copies in the crystallographic asymmetric unit. For the tenth copy, Trp91 is present in the interior, adjacent to the FAD chromophore. Measurement of Trp fluorescence quenching also indicates that Trp91 (the only Trp in Slr1694) changes conformation upon illumination (*5*). Similarly, for the AppA BLUF domain, Jung et al. (*27*) observed a significant movement of the Met side chain adjacent to the Trp residue after light excitation, leading them to propose that the correlated movement of Trp104 and Met106 constitutes the light switch in AppA. For BlrB, ^{15}N-edited NOESY spectra show that Hε1/Nε1 of Trp92 appears to be solvent-exposed in the dark with NOEs only to water (data not shown). This strongly suggests that Trp92 of BlrB is exposed to solvent, consistent with the X-ray crystallographic result (PDB: 2BYC). Trp92 is in close contact with Met94 in BlrB, which is completely conserved among BLUF domains and shows a relatively big change upon light excitation in BlrB. These two interesting residues might be related to the signaling process by reorientating upon illumination.

Integrating data from this study along with prior work, it is clear that BLUF domains experience relatively small conformational changes overall after light activation, mainly electron, proton transfer, and hydrogen bond rearrangement in the immediate vicinity of the FAD (*8, 19, 32*). Several key residues, Tyr9, Asn33, and Gln51, in BlrB play critical roles for the flavin hydrogen-bonding network and nevertheless contribute significantly to the photochemistry. Our observation that mutants of Ala28, Arg32, and Leu66 do not significantly alter the structure and photocycle of BlrB and the limited number of perturbed sites detected upon light excitation suggest that the light-activated signal of BlrB is more likely propagated to its interaction partner from the flavin isoalloxazine ring through its β sheet, not through the two α helices that sandwich FAD. Indeed, our findings suggest that residues on these helices influence the lifetime of the photoexcited state to some degree (*6*). Interestingly, resonance peaks from the entire β_3 strand of BlrB could not be observed in our ^{15}N/^{1}H HSQC and ^{15}N-edited triple resonance spectra, possibly due to line broadening by the dynamical behavior between flavin and amino acids on the β_3 strand. Similar peak disappearance from the triple resonance experiments on β_5 strand of AppA were reported by Grinstead et al. and were similarly suggested to originate from chemical exchange line broadening (*18*).

Structural analysis shows that BLUF domains have strikingly similar structures, go through same photochemistry (10 nm shift), yet can exhibit profound differences in dark state recovery rates. What is the rate-limiting factor for dark state recovery of BLUF domains? How do minimal conformational changes permit light signal propagation that ultimately leads to biological function? Further structural information of light state and light-regulated functional studies and efforts of screening for potential downstream effectors should elucidate the mechanism of the photoreaction and signal transduction for BLUF domains.

ACKNOWLEDGMENT

We thank M. Gomelsky and I. Schlichting for useful discussions of data prior to publication and members of the Gardner laboratory for reviewing the manuscript.

REFERENCES

1. van der Horst, M. A., and Hellingwerf, K. J. (2004) Photoreceptor proteins, "Star actors of modern times": A review of the functional dynamics in the structure of representative members of six different photoreceptor families. *Acc. Chem. Res. 37*, 13–20.
2. Gomelsky, M., and Klug, G. (2002) BLUF: A novel FAD-binding domain involved in sensory transduction in microorganisms. *Trends Biochem. Sci. 27*, 497–500.
3. Anderson, S., Dragnea, V., Masuda, S., Ybe, J., Moffat, K., and Bauer, C. (2005) Structure of a novel photoreceptor, the BLUF domain of AppA from Rhodobacter sphaeroides. *Biochemistry 44*, 7998–8005.
4. Jung, A., Domratcheva, T., Tarutina, M., Wu, Q., Ko, W. H., Shoeman, R. L., Gomelsky, M., Gardner, K. H., and Schlichting, I. (2005) Structure of a bacterial BLUF photoreceptor: insights into blue light-mediated signal transduction. *Proc. Natl. Acad. Sci. U.S.A. 102*, 12350–12355.
5. Yuan, H., Anderson, S., Masuda, S., Dragnea, V., Moffat, K., and Bauer, C. (2006) Crystal structures of the Synechocystis photoreceptor Slr1694 reveal distinct structural states related to signaling. *Biochemistry 45*, 12687–12694.
6. Kraft, B. J., Masuda, S., Kikuchi, J., Dragnea, V., Tollin, G., Zaleski, J. M., and Bauer, C. (2003) Spectroscopic and mutational analysis of the blue-light photoreceptor AppA: a novel photocycle involving flavin stacking with an aromatic amino acid. *Biochemistry 42*, 6726–6734.
7. Zirak, P., Penzkofer, A., Schiereis, T., Hegemann, P., Jung, A., and Schlichting, I. (2006) Photodynamics of the small BLUF protein BlrB from Rhodobacter sphaeroides. *J. Photochem. Photobiol. B 83*, 180–194.
8. Gauden, M., van Stokkum, I. H., Key, J. M., Luhrs, D., van Grondelle, R., Hegemann, P., and Kennis, J. T. (2006) Hydrogen-bond switching through a radical pair mechanism in a flavin-binding photoreceptor. *Proc. Natl. Acad. Sci. U.S.A. 103*, 10895–10900.
9. Takahashi, R., Okajima, K., Suzuki, H., Nakamura, H., Ikeuchi, M., and Noguchi, T. (2007) FTIR study on the hydrogen bond structure of a key tyrosine residue in the flavin-binding blue light sensor TePixD from Thermosynechococcus elongatus. *Biochemistry 46*, 6459–6467.
10. Harper, S. M., Christie, J. M., and Gardner, K. H. (2004) Disruption of the LOV-Jalpha helix interaction activates phototropin kinase activity. *Biochemistry 43*, 16184–16192.
11. Blommel, P. G., and Fox, B. G. (2007) A combined approach to improving large-scale production of tobacco etch virus protease. *Protein Expression Purif. 55*, 53–68.
12. Delaglio, F., Grzesiek, S., Vuister, G. W., Zhu, G., Pfeifer, J., and Bax, A. (1995) NMRPipe: a multidimensional spectral processing system based on UNIX pipes. *J. Biomol. NMR 6*, 277–293.
13. Johnson, B. A. (2004) Using NMRView to visualize and analyze the NMR spectra of macromolecules. *Methods Mol. Biol. 278*, 313–352.
14. Sattler, M., Schleucher, J., and Griesinger, C. (1999) Heteronuclear multidimentional NMR experiments for the structure determination of proteins in solution employing pulsed field gradients. *Prog. NMR Spectrosc. 34*, 93–158.
15. Cornilescu, G., Delaglio, F., and Bax, A. (1999) Protein backbone angle restraints from searching a database for chemical shift and sequence homology. *J. Biomol. NMR 13*, 289–302.
16. Harper, S. M., Neil, L. C., and Gardner, K. H. (2003) Structural basis of a phototropin light switch. *Science 301*, 1541–1544.
17. Kita, A., Okajima, K., Morimoto, Y., Ikeuchi, M., and Miki, K. (2005) Structure of a cyanobacterial BLUF protein, Tll0078, containing a novel FAD-binding blue light sensor domain. *J. Mol. Biol. 349*, 1–9.
18. Grinstead, J. S., Hsu, S. T., Laan, W., Bonvin, A. M., Hellingwerf, K. J., Boelens, R., and Kaptein, R. (2006) The solution structure of the AppA BLUF domain: Insight into the mechanism of light-induced signaling. *ChemBioChem 7*, 187–193.
19. Dragnea, V., Waegele, M., Balascuta, S., Bauer, C., and Dragnea, B. (2005) Time-resolved spectroscopic studies of the AppA blue-light receptor BLUF domain from Rhodobacter sphaeroides. *Biochemistry 44*, 15978–15985.
20. Masuda, S., Hasegawa, K., Ishii, A., and Ono, T. A. (2004) Light-induced structural changes in a putative blue-light receptor with a novel FAD binding fold sensor of blue-light using FAD (BLUF); Slr1694 of Synechocystis sp. PCC6803. *Biochemistry 43*, 5304–5313.

21. Unno, M., Masuda, S., Ono, T. A., and Yamauchi, S. (2006) Orientation of a key glutamine residue in the BLUF domain from AppA revealed by mutagenesis, spectroscopy, and quantum chemical calculations. *J. Am. Chem. Soc. 128*, 5638–5639.
22. Laan, W., Gauden, M., Yeremenko, S., van Grondelle, R., Kennis, J. T., and Hellingwerf, K. J. (2006) On the mechanism of activation of the BLUF domain of AppA. *Biochemistry 45*, 51–60.
23. Lipari, G., and Szabo, A. (1982) Model-free approach to the interpretation of nuclear magnetic resonance relaxation in macromolecules. 1. Theory and range of validity. *J. Am. Chem. Soc. 104*, 4546–4559.
24. Gauden, M., Grinstead, J. S., Laan, W., van Stokkum, I. H., Avila-Perez, M., Toh, K. C., Boelens, R., Kaptein, R., van Grondelle, R., Hellingwerf, K. J., and Kennis, J. T. (2007) On the role of aromatic side chains in the photoactivation of BLUF domains. *Biochemistry 46*, 7405–7415.
25. Masuda, S., Hasegawa, K., and Ono, T. A. (2005) Tryptophan at position 104 is involved in transforming light signal into changes of beta-sheet structure for the signaling state in the BLUF domain of AppA. *Plant Cell Physiol. 46*, 1894–1901.
26. Grinstead, J. S., Avila-Perez, M., Hellingwerf, K. J., Boelens, R., and Kaptein, R. (2006) Light-induced flipping of a conserved glutamine sidechain and its orientation in the AppA BLUF domain. *J. Am. Chem. Soc. 128*, 15066–15067.
27. Jung, A., Reinstein, J., Domratcheva, T., Shoeman, R. L., and Schlichting, I. (2006) Crystal structures of the AppA BLUF domain photoreceptor provide insights into blue light-mediated signal transduction. *J. Mol. Biol. 362*, 717–732.
28. Cuff, J. A., Clamp, M. E., Siddiqui, A. S., Finlay, M., and Barton, G. J. (1998) JPred: A consensus secondary structure prediction server. *Bioinformatics 14*, 892–893.
29. Rost, B., Yachdav, G., and Liu, J. (2004) The PredictProtein server. *Nucleic Acids Res. 32*, W321–W326.
30. Zoltowski, B. D., Schwerdtfeger, C., Widom, J., Loros, J. J., Bilwes, A. M., Dunlap, J. C., and Crane, B. R. (2007) Conformational switching in the fungal light sensor Vivid. *Science 316*, 1054–1057.
31. Masuda, S., Tomida, Y., Ohta, H., and Takamiya, K. (2007) The critical role of a hydrogen bond between Gln63 and Trp104 in the blue-light sensing BLUF domain that controls AppA activity. *J. Mol. Biol. 368*, 1223–1230.
32. Masuda, S., Hasegawa, K., and Ono, T. A. (2005) Light-induced structural changes of apoprotein and chromophore in the sensor of blue light using FAD (BLUF) domain of AppA for a signaling state. *Biochemistry 44*, 1215–1224.
33. Finn, R., Mistry, J., Schuster-Bockler, B., Griffiths-Jone, S., Hollich, V., Lassmann, T., Moxon, S., Marshall, M., Khanna, A., Durbin, R., Eddy, S., Sonnhammer, E., and Bateman, A. (2006) pfam: clans, web tools and services. *Nucleic Acids Res. 34*, 247–251.
34. http://plasma-gate.weizmann.ac.il/Grace/.

BI8011687